# Thermodynamic properties of 3C–SiC

B. Y. Thakore[a)†], S. G. Khambholja[b)], A. Y. Vahora[a)], N. K. Bhatt[a)], and A. R. Jani[a)]

[a)] *Department of Physics, Sardar Patel University, Vallabh Vidyanagar,* 388120, *Gujarat, India*
[b)] *Indus University, Ahmedabad* 380001, *Gujarat, India*

(Received 8 March 2013; revised manuscript received 12 April 2013)

In the present paper, we report on the results of various thermodynamic properties of 3C–SiC at high pressure and temperature using first principles calculations. We use the plane-wave pseudopotential density functional theory as implemented in Quantum ESPRESSO code for calculating various cohesive properties in ambient condition. Further, ionic motion at a finite temperature is taken into account using the quasiharmonic Debye model. The calculated thermodynamic properties, phonon dispersion curves, and phonon densities of states at different temperatures and structural phase transitions at high pressures are found to be in good agreement with experimental and other theoretical results.

**Keywords:** phase transition, phonon dispersion curve, Debye model, thermodynamic property

**PACS:** 64.60.−i, 65.40.De, 65.40.Ba, 65.40.G− **DOI:** 10.1088/1674-1056/22/10/106401

## 1. Introduction

Potential applications of ceramic materials at high temperatures and pressures require understanding of their vibrational and thereby thermodynamic properties.[1] Such a study is also helpful in understanding the bonding mechanism and effects of temperature and/or pressure on various physical properties, which are sensitive to these external influences. Large thermal resistance, high thermal conductivity and strength yet light in weight, high Hugoniot elastic limit, etc. make ceramics, e.g. silicon carbide (SiC), suitable for many technological applications. Gang *et al.*[2] have studied 4H–SiC metal–oxide–semiconductor field-effect transistors (MOSFETs) with high purity semi-insulating substrates and Wang *et al.*[3] have fabricated the Schottky barrier diodes by chemical vapor deposition using epitaxial layers of SiC. Previously, many researchers have carried out studies of various physical properties including the detailed study of intrinsic defects and polytypic transition of zincblende (3C, ZB) SiC and its polytypes using different experimental techniques.[4–11] Theoretically, various ground state and high pressure and temperature properties for different polytypes of SiC have also been studied.[12–24] For instance, Vardachari *et al.*[12] have studied some thermodynamic properties of SiC using full-potential linearized augmented plane-wave (FP-LAPW) method within the harmonic approximation (HA). They have used PHONON program to calculate phonon dispersion relation, and thereby the free energies at elevated temperatures. Although the harmonic approximation works well at low temperatures ($T < \theta_D$; the Debye temperature), it has some limitations at higher temperatures. In particular, the HA fails to predict volume thermal expansion, temperature dependencies of elastic constants, and phonon frequencies. Karch *et al.*[24,25] have studied the structural, lattice dynamical and thermal properties of cubic SiC using density functional theory within the local density approximation (LDA). They have calculated cohesive properties in ambient condition using plane-wave density functional theory, while high-$T$ thermodynamic properties were calculated within the quasiharmonic approximation (QHA) using the full phonon density of states (p-DOS). On the other hand, Vashishtha *et al.*[15] have proposed an effective potential comprised of two-body and three-body interactions. The two-body interaction was designed to take care of electrostatic Coulomb's interaction and Van der Waals dipole–dipole interaction, while the covalent characteristic of the sample was modeled through the three-body part of the potential. Using the molecular dynamics (MD) technique, these authors have studied structural, elastic, and dynamical properties of SiC in three phases; namely crystalline 3C–SiC, amorphous, and liquid states, at different densities and temperatures.

Another strong candidate for the calculation of low–to–high temperature free energies over a wide range of densities is the coupling parameter series expansion (CPSE) thermodynamic perturbation theory (TPT) and non-hard sphere perturbation strategy as employed by Zhou.[26–29] In the series of papers, the author has elegantly proved and verified the applicability of the higher order series expansion of free energy perturbation theory by formulating a new perturbation framework differing from the traditional high temperature perturbation expansion framework. Robustness of the approach was justified through the accurate results for various thermodynamic properties ranging from critical point to far from critical point. Particularly, Zhou theory[28] predicts with pretty high accuracy the free energies for extremely short-range square well fluid with reduced temperature as low as 0.235 where traditional liquid state theories disappointingly cease to be effec-

†Corresponding author. E-mail: brijmohanthakore@rediffmail.com

© 2013 Chinese Physical Society and IOP Publishing Ltd 

tive for such a limiting case. In a summative paper of the series of work, the author[29] has proved and verified that the CPSE provides an elegant solution to a long-term outstanding problem, i.e., the estimation of high-order coefficients of the traditional high temperature series expansion by Zwanzig.[30] Considering the general application of the Zwanzig theory in calculating liquid and solid thermodynamic properties, one expects that the Zhou theory can also be extended to the solid state area.

Considering the scattered nature of all previous findings and various techniques to evaluate the free energies, and also the need for comprehensive thermal properties up to melting temperature, it seems very necessary to investigate the vibrational response and high temperature thermodynamics of technologically important cubic SiC. In the present study, various ground state cohesive properties are computed using plane-wave pseudopotential density functional theory (DFT). Although a very similar approach has been used by Karch *et al.*[24,25] the present calculations differ in two considerations: (i) the treatment for ionic free energy, and (ii) the exchange and correlation functional. In Refs. [24] and [25], the free energy due to lattice vibrations was computed using the complete p-DOS within the QHA, while we have treated the ionic motions at high temperatures using the quasiharmonic Debye model as implemented in GIBBS code.[31] Secondly, we have rather employed the generalized gradient approximation (GGA) for exchange and correlation effects, which we believe is the proper choice for such a covalent $sp^3$ bonded material. Using the linear response theory, we also report on the quasiharmonic phonon dispersion curves (PDCs) and p-DOS for 3C–SiC in high temperature and pressure conditions. The results are in excellent agreement with experimental phonon frequencies.

## 2. Theory

The silicon carbide crystallizes into ZB structure in ambient condition. The Si and C atoms occupy positions (0,0,0) and (0.25,0.25,0.25), respectively, in an fcc primitive cell having the space group of $F4\bar{3}m$. To calculate the total energy of ZB–SiC, a self-consistent density functional scheme[32] was used. In the literature, the exchange correlation energy in DFT has been defined by local density approximation (LDA)[33] for the system having uniform electron charge density. But for the system of non-uniform charge density, the exchange–correlation energy by LDA has been corrected by the gradient of charge density using different versions of a generalized gradient approximation (GGA). In the present study we therefore take a norm conserving pseudopotential with nonlinear core correction within the GGA to solve the Kohn–Sham energy functional. The calculation is performed in steps of 0.1 a.u., and the convergence test gives an $8\times8\times8$ Monkhorst–Pack (MP) $\boldsymbol{k}$-point grid[34] for Brillouin-zone (BZ) sampling along with the kinetic energy cutoff as 165 Ry. This ensures the convergence of total energy to 0.01 mRy.

Phonon dispersion curves are obtained employing the linear response theory within the density functional perturbation theory (DFPT). In this scheme, the second-order derivatives of the self-consistent total energies with respect to atomic positions (i.e., atomic force constants) are used in calculating the dynamical matrix, while considering the external potential as a perturbation. In the present computation, BZ sampling is performed with a line-width of 0.05 Ry. A $4\times4\times4$ $\boldsymbol{k}$-point mesh is used for the interpolation of force constants. Finally, the dynamical matrices are calculated on this grid, and the $r$-space force constants are obtained by inverse Fourier transform.

For a cubic structure, there are only three independent elastic stiffness constants: $C_{11}$, $C_{12}$, and $C_{44}$, which are determined from the long wavelength limit of phonon frequencies along [100] and [110] planes.[24] The slope of the phonon frequencies in the long wavelength limit gives the corresponding sound velocities, from which elastic constants can be determined using the following relations:

$$C_{11}=\rho v_{\mathrm{L}}^2[100],\quad C_{44}=\rho v_{\mathrm{T}}^2[100],$$
$$C_{11}-C_{12}=2\rho v_{\mathrm{T1}}^2[110]. \tag{1}$$

Here, $\rho\equiv1/V$ is the bulk mass density, $v_{\mathrm{L}}$ and $v_{\mathrm{T}}$ are longitudinal and transverse sound velocities, respectively, and $V$ is the volume. The isothermal bulk modulus is calculated using the following relation:

$$B_0=\frac{C_{11}+2C_{12}}{3}. \tag{2}$$

The Poisson ratio ($\sigma$) in the present calculation is calculated using the expression as given in Ref. [15]. These results are also listed in Table 1.

**Table 1.** Calculated structural and elastic properties of SiC in ZB phase along with corresponding experimental and theoretical values.

| Properties | Present | Exp. | Others |
|---|---|---|---|
| $a_0$/Å | 4.364 | 4.3596[f] | 4.3581[b], 4.385[a], 4.359[c], 4.344[d] |
| $B_0$/GPa | 222.95 | 225[g] | 225.1[b] , 224[c], 222[d] |
| $B_0'$ | 3.99 | — | 4.16[c] |
| $E_c$/(eV/atom) | −6.1434 | −6.34[e] | −6.48[a], −6.3410868[b] |
| $C_{11}$/GPa | 380 | 390[g] | 390.1[b] , 382[c], 390[d] |
| $C_{12}$/GPa | 147.8 | 142[g] | 142.7[b] , 145[c], 134[d] |
| $C_{44}$/GPa | 237 | 256[g] | 191[b], 240[c], 253[d] |
| Poisson ratio ($\sigma$) | 0.28 | 0.267[g], 0.168[h] | 0.268[b] |

[a]Ref. [12], [b]Ref. [15], [c]Ref. [16], [d]Ref. [24], [e]Ref. [35], [f]Ref. [42], [g]Ref. [43], [h]Ref. [44]

Further, the pressure-induced structural phase transition (SPT) in SiC from ZB to rock salt (RS) structure is also reported based on the calculation of total enthalpies of both phases. Enthalpy at 0 K temperatures is written as

$$H(P,V)=E(V)+VP(V), \tag{3}$$

where the first term on the right indicates the total energy and $P(V)$ is the corresponding pressure. The total energy of RS structure is also calculated using the plane-wave pseudopotential within the DFT–GGA.

To investigate high temperature thermodynamics, we use the quasiharmonic Debye model.[31] The basic assumption used in the model is the replacement of the true phonon density of state $g(\omega)$ by $\sim \omega^2$ term. For example, the low frequency part of p-DOS is indeed a quadratic in $\omega^2$. In this model, the non-equilibrium Gibbs function is given by[31]

$$G^*(V;P,T) = E(V) + VP(V) + A_{\rm vib}(\theta(V),T), \tag{4}$$

where the first term on the right represents the optimized total energy of a material, which is calculated using the self-consistent plane-wave pseudopotential formalism. The last term contains the contribution of lattice vibrations at finite temperatures to the total free energy. It is given by

$$A_{\rm vib}(\theta(V),T) = nk_{\rm B}T\Big[\frac{9}{8}\frac{\theta(V)}{T} + 3\ln\big(1-{\rm e}^{-\theta(V)/T}\big) - D\Big(\frac{\theta(V)}{T}\Big)\Big]. \tag{5}$$

Here, $D(\theta(V)/T)$ is the Debye integral,

$$D(y) = \frac{3}{y^3}\int_0^y \frac{x^3}{{\rm e}^x - 1}\,{\rm d}x, \tag{6}$$

where $y = \theta(V)/T$, $\theta(V)$ is the volume-dependent Debye temperature, and $n$ is the number of atoms per formula unit.

The Debye characteristic temperature of the solid, $\theta(V)$ in Eq. (4), is related to an average sound velocity, since in Debye's theory the vibrations of the solid are considered as elastic waves. Assuming an isotropic solid, with Poisson ratio $\sigma$,[15] $\theta(V)$ is given by

$$\theta(V) = \frac{\hbar}{k_{\rm B}}[6\pi^2 V^{1/2} n]^{1/3} f(\sigma)\sqrt{\frac{B_{\rm s}}{M}}, \tag{7}$$

where $M$ is the molecular mass per formula unit, $B_{\rm s}$ the adiabatic bulk modulus, and $f(\sigma)$ is given by

$$f(\sigma) = \Big\{3\Big[2\Big(\frac{2(1+\sigma)}{3(1-2\sigma)}\Big)^{3/2} + \Big(\frac{(1+\sigma)}{3(1-\sigma)}\Big)^{3/2}\Big]^{-1}\Big\}^{1/3}.$$

Thus, our calculation does not involve any experimental data as input. All necessary ingredients to Eq. (5) are calculated using the present *ab initio* calculations. Once we have total free energy as an explicit function of temperature and pressure, equilibrium properties at different temperatures are calculated by following the zero pressure condition. First, the volume thermal expansion being one of the most important quantities related to the anharmonicity of a material is obtained up to 3000 K.

As a further test of the present calculations, we obtain the isothermal ($B_{\rm T}$) and adiabatic ($B_{\rm s}$) bulk moduli at elevated temperatures as

$$B_{\rm T}(p,T) = \Big[V\Big(\frac{\partial^2 G^*(V;p,T)}{\partial V^2}\Big)_{p,T}\Big]_{V_{\rm eq}(p,T)} \quad \text{and}$$
$$B_{\rm s} = B_{\rm T}(1+\alpha\gamma T). \tag{8}$$

Here, $\alpha$ is the coefficient of thermal expansion, $V_{\rm eq}$ is the equilibrium volume and $\gamma$ is the thermodynamic Grüneisen parameter, which is defined as

$$\gamma = -\frac{{\rm d}\ln\theta(V)}{{\rm d}\ln(V)}. \tag{9}$$

## 3. Results and discussion

The cohesive energy at various lattice constants is calculated by subtracting energy of an isolated free atom from the total energy of the bulk, and is shown in Fig. 1 along with the reported first principles and experimental data. The present estimate of cohesive energy, −6.1434 Ry, is in excellent agreement with the experimental datum −6.34 Ry[35] as well as with the other theoretical results: −6.48 Ry[12] and −6.3410868 Ry.[15] Further, in order to estimate equilibrium lattice constant ($a_0$), isothermal bulk modulus ($B_0$), and its first-order pressure derivative ($B_0'$), the calculated cohesive energies are fitted to Murnaghan equation of state[36] and the results are compared in Table 1. As shown in Table 1, the close agreement with the experimental results of various cohesive properties by the present calculation as compared with those given by Karch *et al.*[24] is attributed to the use of GGA. In such tetrahedrally coordinated covalent materials, one cannot expect a spherically symmetric potential[15] and the electronic charge distribution is highly angular. To take into account the effect of inhomogeneous electron cloud, one must retain gradient corrections to the exchange and correlation functional.

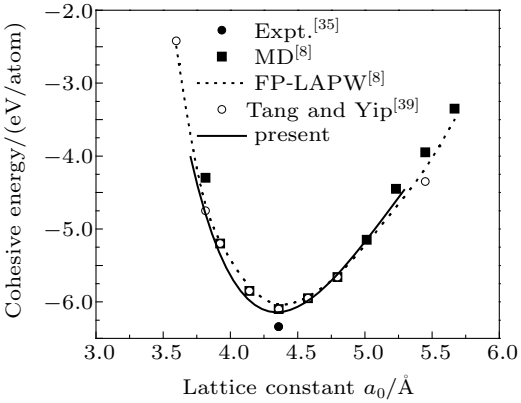



**Fig. 1.** Cohesive energy curves of 3C–SiC with available results.

The calculated values of PDC are shown in Figs. 2 and 3 at various pressures and temperatures, respectively, in excellent agreement for both acoustic and optical phonons with the experimental results presented by Serrano *et al.*[9] in ambient condition. The lighter C atom contributes to p-DOS only at

higher frequencies. The p-DOSs at various pressures and temperatures, respectively, are also shown in Figs. 4 and 5. We have noticed that the frequency corresponding to the principal peak and its magnitude in computed p-DOS (in ambient condition) coincide with experimental[15] and theoretical results.[23] Excellent agreement of the present PDC and p-DOS with experimental results thus confirms the use of plane-wave pseudopotential in examining the vibrational response of the material.

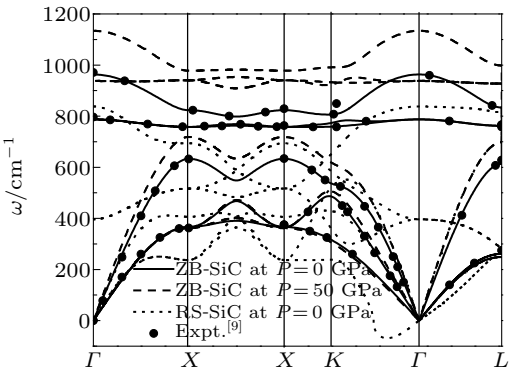



**Fig. 2.** Phonon dispersions relations along major symmetry directions for 3C–SiC.

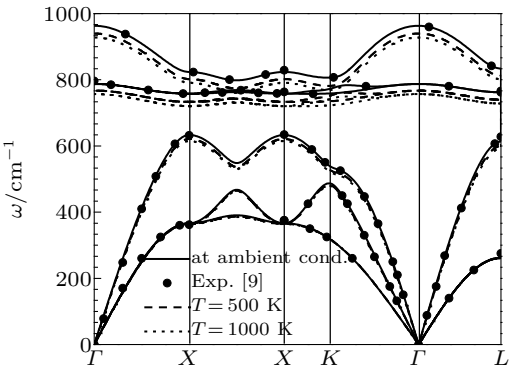



**Fig. 3.** Phonon dispersion relations along major symmetry directions for 3C–SiC.

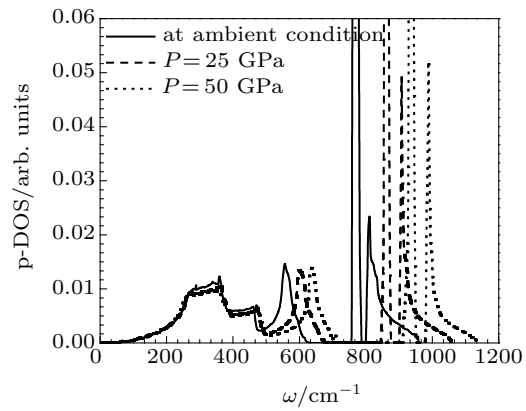



**Fig. 4.** Computed phonon densities of states with various pressures.

The calculated enthalpies of both phases are shown in Fig. 6. We obtain phase transition pressure to be 70 GPa, which is in good agreement with previously reported theoretical result (66 GPa)[37] but lower than the experimental finding (100 GPa).[10] However, it should be emphasized that the experimental phase transition pressure is calculated for forward transition and requires excess value of pressure beyond equilibrium. To analyze the conflict, we also examine the PDCs and p-DOSs at different pressures in Figs. 2 and 4. It is evident from the figures that upon compression, the phonon modes turn harder for longitudinal branches along all symmetry directions, while the transverse phonon frequencies along [100] plane and [111] plane become softer. The first transverse branch (T1) along the [110] plane turns harder upon compression but the second (T2) branch becomes softer. This process is continued to higher pressures and eventually ZB structure collapses into RS structure due to the softening of T2 phonons. In contrast, we also find that at zero pressure, the T2 mode in [110] plane of RS–SiC shows imaginary phonon frequency but increases with pressure increasing. Thus, in ambient condition the RS phase is unstable. Hence we conclude that the softening mechanism for the transverse phonon frequencies along [110] plane is responsible for SPT from ZB to RS structure. Regarding the p-DOSs at high pressures, we observe that the peak of p-DOS shows shifts towards the higher frequency side, showing hardening in peak frequency upon compression.

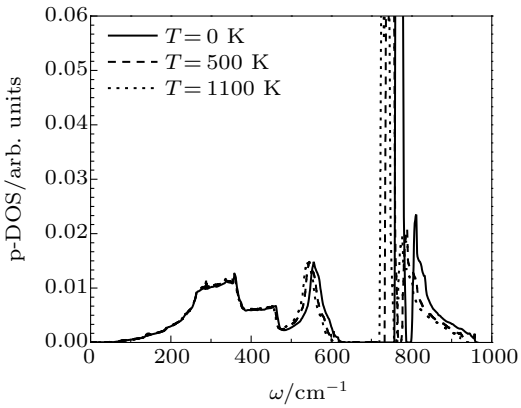



**Fig. 5.** Calculated quasi-harmonic phonon densities of states.

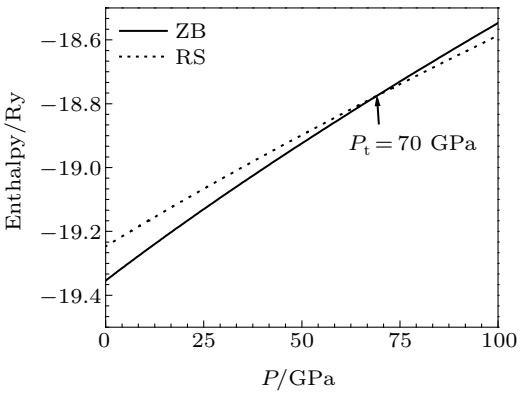



**Fig. 6.** Enthalpy-pressure curves for ZB and RS structured SiC.

Results for lattice constant ($a_0$) as a function of temperature are shown in Fig. 7 along with the literature data. We can

see a good accordance of the present findings with experimental results and the MD results[15] up to melting temperature ($T_m = (3100 \pm 40)$ K).[38] Maximum deviation of the present calculated lattice constants is just 3% for the entire temperature range. It should be mentioned that Vashistha *et al.*[15] have used classical molecular dynamics through using the modified Stillinger–Weber form of potential, while we use the classical Debye model to compute free energies at elevated temperatures. The calculated lattice parameters at various temperatures are used to calculate phonon frequencies of SiC as shown in Figs. 3 and 5. The effect of the temperature is to uniformly lower the phonon frequencies in both longitudinal and transverse modes. For example, if we identify the frequency corresponding to the peak in p-DOS as a characteristic frequency, it decreases with temperature increasing, the so-called phonon frequency shift. However, the decrease in frequency with temperature increasing is small, which indicates that the temperature coefficient of elastic constant should also be small. Also, the peak in the p-DOS shifts towards the lower frequency, while the height of p-DOS slightly decreases with temperature increasing, leaving the gross structure of p-DOS almost unchanged. These observations indicate that the geometric mean frequency of lattice vibration decreases with temperature increasing, indicating weak correlation among atoms at high temperature. This validates the use of a classical approach at temperatures higher than the characteristic temperature. It needs to be mentioned that we have not found any signatures of structural phase transition for the entire range of temperature, and ZB structure is found to be stable up to the highest temperature that is investigated.

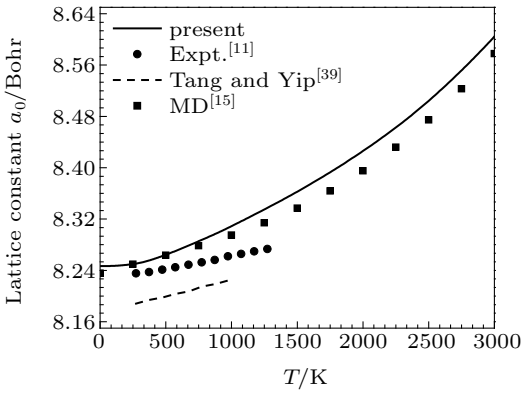



**Fig. 7.** Equilibrium lattice constants at various temperatures.

Shown in Fig. 8 are the results for bulk moduli at different temperatures along with the previous results.[25,39,40] It is obvious that due to thermal expansion, the bulk moduli decrease at higher temperatures. The discrepancy between the present observed results and those presented by Karch *et al.*[25] may be attributed to the different treatments for exchange and correlation functional. These authors have used LDA, which we believe, is an over simplified view for such tetrahedrally bonded ceramics in calculating thermal expansion. They found low thermal expansion coefficient compared with the experimental one, which causes the crystal to stiffen even when temperature is raised. Hence, decrease in bulk modulus with temperature increasing is less prominent in their study. Secondly, for the temperature range of interest ($T > \theta_D$), their calculated value of thermodynamic Grüneisen parameter ($\gamma$) is almost constant. We strongly believe that as a measure of anharmonicity it should be temperature-sensitive, at least above the Debye temperature.

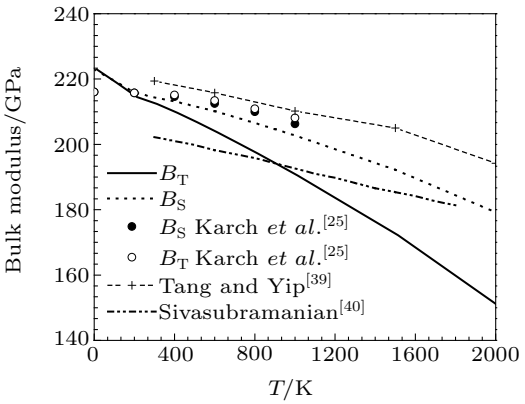



**Fig. 8.** Present calculated bulk moduli along with other available results.

Figure 9 shows the temperature dependencies of Debye temperature for cubic SiC. We have used the classical approach of quasi-harmonic Debye model for calculating the thermal contribution of lattice ions. As a result, we do not observe any quantum effects present at low temperatures ($T < \theta_D$). However, we obtain the correct trend, i.e., decrease in $\theta_D$ with temperature increasing due to decrease in phonon frequency. Since the results of Vashishtha *et al.*[15] are limited to $T < \theta_D$, it is difficult to compare the two studies. They have calculated Debye temperature using the well-known low temperature expression of Debye temperature in terms of specific heat, which is given by

$$C_v = \frac{12}{5}\pi^4 N k_B (T/\theta(D))^3.$$

However, it is worth noting that the empirically derived results[41] clearly show a downward trend above $T = 700$ K, justifying our prediction for higher temperatures. We should point out that the scale on $\theta_D$ axis in $\theta_D \to T$ graph in Ref. [15] may be an order of magnitude higher, as references [15] and [41] have both used the same source (i.e., $C_v$) for calculating $\theta_D$. Further, the trends observed in both the derived results are also different. This clearly manifests the sensitivity of the Debye temperature to temperature. In such conflicts, we strongly recommend model-free investigation of $\theta_D$ at higher temperatures.

Finally, specific heats at constant volume ($C_v$) and pressure ($C_p$) are plotted in Fig. 10 along with the molecular dynamics results.[15] The present computed values of $C_v$ are

found in good agreement with the MD results. Their slight discrepancies may be due to the overestimation of thermal expansion and rather rapid decrease in bulk modulus above the Debye temperature.

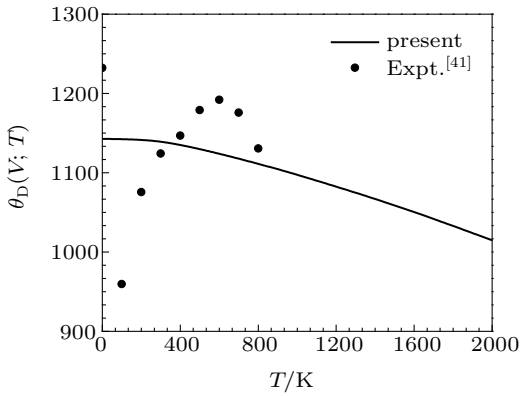



**Fig. 9.** Calculated and measured Debye temperatures each as a function of temperature.

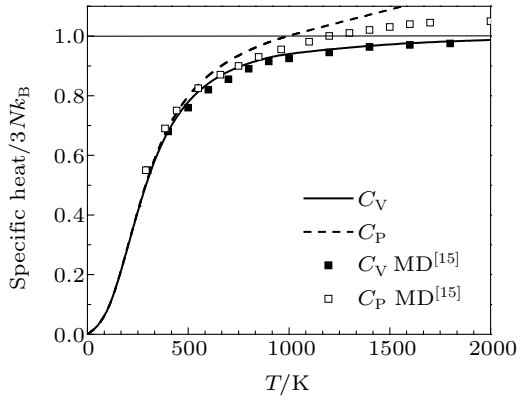



**Fig. 10.** Calculated specific heats each as a function of temperature. Horizontal line indicates the Dulong–Petit limit.

## 4. Conclusions

In this paper, we calculate various thermodynamic properties of 3C–SiC using self-consistent plane-wave pseudopotential formalism within the GGA. Density functional perturbation theory is used to deduce phonon dispersions and vibrational densities of states within the QHA at different pressures and temperatures. Satisfactory prediction of various physical properties and PDCs in ambient condition justifies the use of pseudopotentials within the GGA even for such materials exhibiting directional covalent bonding. On the other hand, MD simulation technique requires a prior knowledge of pair potential, whose parameters are usually determined by fitting some of the experimental properties. Unlike the MD approach, the present approach differs in calculating total energy by solving KS functional self-consistently and does not require any experimental inputs. Further, the present study suggests that the SPT in SiC is due to elastic instability. Previous study[10] has identified bond ordering in 3C–SiC as the phonon softening mechanism. Phonon softening along the transverse mode in (110) plane at the zone center ($\Gamma$-point) of Brillouin-zone is the precursor of transformation of ZB into RS structure. Also, high temperature thermodynamic properties are studied using the quasiharmonic Debye model through using the present first principles cohesive properties as the only input. The simplification involved in the Debye model is valid for moderately high temperatures (e.g., close to melting temperature), where thermal excitation energy (or equivalent frequency) is relatively low. It seems that the use of QHA (i.e., ignoring higher order terms in the free energy expansion) is adequate. For example, volume thermal expansion, temperature-dependent bulk moduli, specific heats, and characteristic temperature all show the correct trend in the $T > \theta_D$ regime. For the entire temperature range $C_p$ is found to be greater than $C_v$, which implies the thermodynamic stability of the crystal. Consequently we believe that the present high-$T$ results for various thermal properties may serve as a reliable means of comparison in future study for example, to resolve the discrepancy in high-$T$ behavior of Debye temperature.

## Acknowledgment

The author A. Y. Vahora acknowledges the financial support of UGC, New Delhi, India. Also, we are thankful to pwscf developers and developers of GIBBS program.

## References

[1] Hao A, Yang X, Wang X, Zhu Y, Liu X and Liu R 2010 *J. Appl. Phys.* **108** 063531
[2] Chen G, Bai S, Li Z Y, Wu P, Chen Z and Han P 2009 *Chin. Phys. B* **18** 4474
[3] Wang Y H, Zhang Y M, Zhang Y M, Zhang L, Jia R X and Chen D 2010 *Chin. Phys. B* **19** 036803
[4] Ping C, Zhang Y M, Zhang Y M and Hui G 2010 *Chin. Phys. B* **19** 097802
[5] Yang Y T, Han R and Wang P 2008 *Chin. Phys. B* **17** 3459
[6] Boulle A, Aube J, Galben-Sandulache I G and Chaussende D 2009 *Appl. Phys. Lett.* **94** 201904
[7] Snead L L, Nozawa T, Katoh Y, Byun T S, Kondo S and Petti D A 2007 *J. Nucl. Mater.* **371** 329
[8] Ivashchenko V I, Turchi P E A and Shevchenko V I 2009 *Phys. Rev. B* **75** 085209
[9] Serrano J, Strempfer J, Cardona M, Böhning M S, Requardt H, Lorenzen M, Stojetz B, Pavone P and Choyke W J 2002 *Appl. Phys. Lett.* **80** 4360
[10] Yoshida M, Onodera A, Ueno M, Takemura K and Shimomura O 1993 *Phys. Rev. B* **48** 10587
[11] Li Z and Bradt R C 1986 *J. Mater. Sci.* **21** 4366
[12] Varadachari C and Bhowmick R 2009 *Modelling Simul. Mater. Sci. Eng.* **17** 075006
[13] Xiao H Y, Gao F, Zu X T and Weber W J 2009 *J. Phys.: Condens. Matter* **21** 245801
[14] Xiao H Y, Gao F, Wang L M, Zu X T, Zhang Y and Weber W J 2008 *Appl. Phys. Lett.* **92** 241909
[15] Vashishtha P, Kalia R K, Nakano A and Rino J P 2007 *J. Appl. Phys.* **101** 103515
[16] Erhart P and Albe K 2005 *Phys. Rev. B* **71** 035211
[17] Durandurdu M 2004 *J. Phys.: Condens. Matter* **16** 4411
[18] Prikhodko M, Miao M S, Lambrecht W R L 2002 *Phys. Rev. B* **66** 125201

[19] Shimojo F, Ebbsjo I, Kalia R K, Nakano A, Rino J P and Vashishta P 2000 *Phys. Rev. Lett.* **84** 3338

[20] Karch K, Bechstedt F, Pavone P and Strauch D 1996 *J. Phys.: Condens. Matter* **8** 2945

[21] Karch K, Bechtedt F, Pavone P and Strauch D 1996 *Phys. Rev. B* **53** 13400

[22] Talwar D N and Sherbondy J C 1995 *Appl. Phys. Lett.* **67** 3301

[23] Hofmann M, Zywietz A, Karch K and Bechstedt F 1994 *Phys. Rev. B* **50** 13401

[24] Karch K, Pavone P, Windl W, Schutt O and Strauch D 1994 *Phys. Rev. B* **50** 17054

[25] Karch K, Pavone P, Windl W, Strauch D and Bechstedt F 1995 *Int. J. Quantum Chem.* **56** 801

[26] Zhou S 2006 *Phys. Rev. E* **74** 031119

[27] Zhou S 2009 *J. Chem. Phys.* **130** 054103

[28] Zhou S 2011 *J. Stat. Mech.* P09001

[29] Zhou S 2011 *AIP Advances* **1** 040703; and references therein

[30] Zwanzig R W 1954 *J. Chem. Phys.* **22** 1420

[31] Blanco M A, Franscisco E and Luana V 2004 *Comput. Phys. Commun.* **158** 57 and references therein

[32] Giannozzi P, Baroni S, Bonini N, Calandra M, Car R, Cavazzoni C, Ceresoli D, Chiarotti G L, Cococcioni M, Dabo I, Corso A D, Gironcoli S, Fabris S, Fratesi G, Gebauer R, Gerstmann U, Gougoussis C, Kokalj A, Lazzeri M, Martin-Samos L, Marzari N, Mauri F, Mazzarello R, Paolini S, Pasquarello A, Paulatto L, Sbraccia C, Scandolo S, Sclauzero G, Seitsonen A P, Smogunov A, Umari P and Wentzcovitch R M 2009 *J. Phys.: Condens. Matter* **21** 395502

[33] Perdew J P and Wang Y 1992 *Phys. Rev. B* **45** 13244

[34] Monkhorst H J and Pack J D 1976 *Phys. Rev. B* **13** 5188

[35] Auciello O, Birrell J, Carlisle J A, Gerbi J E, Xiao X, Peng B and Espinosa H B 2004 *J. Phys.: Condens. Matter* **16** R539

[36] Murnaghan F D 1944 *Proc. Natl. Acad. Sci. USA* **30** 244

[37] Chang K J and Cohen M L 1987 *Phys. Rev. B* **35** 8196

[38] Franke P and Neuschütz D (eds.), Vol. **19B2** C–Si *Springer Materials — The Landolt–Börnstein Database* DOI:10.1007/10757405_45

[39] Tang M and Yip S 1995 *Phys. Rev. B* **52** 15150

[40] Sivasubramanian K, Raju S and Monadas E 2001 *J. Eur. Ceram. Soc.* **21** 1229

[41] Gurvich V L and Veyts I V 1972 *Thermodynamic Properties of Individual Substances* (New York: Hemisphere Publishing Corporation)

[42] http://www.ioffe.ru/SVA/NSM/ (Ioffe Institute, 2003)

[43] Feldman D W, Parker J H, Choyke W J and Patrick L 1968 *Phys. Rev.* **173** 787

[44] Carnahan R D 1968 *J. Am. Ceram. Soc.* **51** 223